Bulletin of Electrical Engineering and Informatics
Vol. 10, No. 2, April 2021, pp. 848∼855
ISSN: 2302-9285, DOI: 10.11591/eei.v10i2.2117

Studying strictly positive secure capacity in cognitive radio-based non-orthogonal multiple access

Chi-Bao Le, Dinh-Thuan Do
Faculty of Electronics Technology, Industrial University of Ho Chi Minh City (IUH), Ho Chi Minh City, Vietnam

Article Info

Article history:

Received Oct 16, 2020
Revised Jan 7, 2021
Accepted Feb 16, 2021

Keywords:

Cognitive radio
NOMA
Strictly positive secure capacity

ABSTRACT

This paper studies a downlink security-aware secure outage performance in the secondary network of cognitive radio-assisted non-orthogonal multiple access network (CR-NOMA). The multiple relay is employed to assist transmission from the secondary source to destinations. The security-aware performance is subject to constraints in fixed power allocation factor assigned to each secondary user. The security-aware secure performance is based on channel state information (CSI) at the physical layer in which an eavesdropper intends to steal information. According to the considered system, exact expressions of Strictly positive secure capacity (SPSC) are proved to analyze system in terms of secure performance. Finally, the secondary user secure problem is evaluated via Monte-Carlo simulation method. The main results indicate that the secure performance of proposed system can be improved significantly.

Corresponding Author:

Dinh-Thuan Do
Faculty of Electronics Technology, Industrial University of Ho Chi Minh City
12 Nguyen Van Bao Road, Go Vap District, Ho Chi Minh City, Vietnam
Email: dodinhthuan@iuh.edu.vn

1. INTRODUCTION

Both non-orthogonal multiple access (NOMA) and physical-layer security (PLS) have been introduced as promising enabling technologies to implement some applications for Internet of Things (IoT) or future systems [1-4]. Recently, the coexistence of these two important communication techniques benefits from cognitive ability and massive connections and these hybrid techniques have been considered to provide spectral efficient improvement for wireless transmission such as recent work [6-8].

Furthermore, physical-layer security (PHY) has attracted great interests while wireless applications are more popular. PHY based secure method does not require extra resources for the secret key [10-14]. In order to achieve secure communication, one can exploit the physical layer characteristics of the wireless channels. However, the secrecy rate of wireless communication systems is constrained by the channel state information [15]. In order to improve the secrecy rate, many methods are introduced such as jamming, multiple antennas, cooperative relaying and artificial noise (AN)-aided techniques have been studied [16]. Main results reported in [17-24] that these techniques benefit to improve the secrecy rate.

Interestingly, most existing works have mainly focused on the performance and optimization of the PLS in NOMA systems . However, there is still open problems to rigorously study the feasibility of achieving the better secure performance by using best relay selection in secondary network of CR-NOMA systems. Although the joint user scheduling and power allocation problems are investigated for NOMA-based wireless network in [17], how cognitive radio technology affects the secure performance for NOMA-based wireless network needs further studies. In this paper, we study the security-aware SPSC metric CR-NOMA network.

2. SYSTEM MODEL

In Figure 1, we consider the CR system containing the secondary network including base station (BS). To enhance performance of distance users, we need N relay nodes. Regarding distance users, two destination U_1, U_2, one eavesdropper E are considered their performance. Through the paper, h_u is denoted as channel for node u, and it follows Rayleigh fading model with channel gain λ_u. It is noted that P_S is transmit power at BS and it is limited under constraint with the primary network which contains primary destination P_D. The interference channel from BS to the primary network is h_{SP}. h_{R_n} is the channel between BS and R. h_{R_n} is denoted as the channel between relay and U_i.

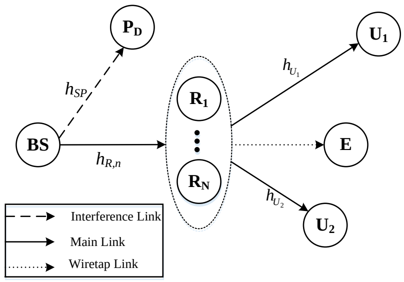

Figure 1. Secure CR-NOMA system

In CR-NOMA, the transmit power at the BS is constrained by (1)

$$P_S \leq \min\left(\frac{I}{|h_{SP}|^2}, \bar{P}_S\right) \tag{1}$$

in which, we call $\bar{P}_S$ and I as maximum average transmit power at the BS and interference temperature constraint (ITC) at primary destination P_D, respectively. At the first hop transmission, the n-th node among N relay node, the received signal can be formulated by (2)

$$y_R = h_{R_n}\left(\sqrt{a_1 P_S}x_1 + \sqrt{a_2 P_S}x_2\right) + n_{R_n} \tag{2}$$

where the AWGN noise terms at R is n_{R_n}. Regarding the relay is used to forward signal, the criteria to select relay with its index, i.e. n^* is formulated related the best channel

$$n^* = \arg \underbrace{\max}_{1,2,\ldots,N} |h_{R_n}|^2 \tag{3}$$

To decode signal x_1 and x_2 at R, the signal-to-interference-plus-noise ratio (SINR) is given by (4).

$$SNR_R^1 = \frac{a_1\rho_S|h_{R_n}|^2}{a_2\rho_S|h_{R_n}|^2 + 1} \tag{4}$$

where $\rho_S = \frac{P_S}{\sigma^2}$ is the transmit signal to noise ratio (SNR) at the BS. At relay relying SIC, it is necessary to examine the received SNR at R to detect message x_2 as (5).

$$SNR_R^2 = a_2\rho_S|h_{Rn}|^2 \tag{5}$$

In the next phase, the link netween selected relay R_n and $U_i, i = 1, 2$ is required to proceed signal $\sqrt{a_1 P_R}\bar{x}_1 + \sqrt{a_2 P_R}\bar{x}_2$. P_R is called as the transmit power at R. The received signal U_i is expressed by (6)

$$y_{U_i} = h_{U_i}\left(\sqrt{a_1 P_R}\bar{x}_1 + \sqrt{a_2 P_R}\bar{x}_2\right) + n_{U_i} \quad, \forall i \in \{1, 2\} \tag{6}$$

in which the AWGN noise terms is n_{U_i} measured at U_i. Further, principle of NOMA applied to U_i with higher power factor, it can detect $\bar{x}_1$ by considering $\bar{x}_2$ as a background noise with (7)

$$SNR_{U_1} = \frac{a_1 \rho_R |h_{U_1}|^2}{a_2 \rho_R |h_{U_1}|^2 + 1} \tag{7}$$

where $\rho_R = \frac{P_R}{\sigma^2}$ is the transmit SNR at R. To continue detecting procedure, U_2 needs SIC to decode $\bar{x}_1$ while considering its own data $\bar{x}_2$ as a noise. The SINR is written as (8).

$$SNR_{U_2,x_1} = \frac{a_1 \rho_R |h_{U_2}|^2}{a_2 \rho_R |h_{U_2}|^2 + 1} \tag{8}$$

In this regard, U_2 detects its own signal and the corresponding SNR is given as (9).

$$SNR_{U_2,x_2} = a_2 \rho_R |h_{U_2}|^2 \tag{9}$$

Unfortunately, eavesdropper steals information from the selected relay, the received signal at E is given as (10)

$$y_E = h_E \left(\sqrt{a_1 P_E} \bar{x}_1 + \sqrt{a_2 P_E} \bar{x}_1 \right) + n_E \tag{10}$$

where n_E is the AWGN noise terms at E. The channel between Relay and E is h_E. Then, SNR at E is given as

$$SNR_{Ei} = a_i \rho_E |h_E|^2 \quad , i \in \{1, 2\} \tag{11}$$

where $\rho_E = \frac{P_E}{\sigma^2}$ is transmit SNR at E. The secrecy capacity for U_1, U_2 are computed respectively as

$$C_1 = \left[\frac{1}{2} \log_2 \left(\frac{1 + \min \left(SNR_R^1, SNR_{U_1} \right)}{1 + SNR_{E_1}} \right) \right]^+, \tag{12}$$

$$C_2 = \left[\frac{1}{2} \log_2 \left(\frac{1 + \min \left(SNR_R^2, SNR_{U_2,x_2} \right)}{1 + SNR_{E_2}} \right) \right]^+, \tag{13}$$

where $[x]^+ = \max [x, 0]$.

3. SPSC ANALYSIS

3.1. SPSC computation at U_1

We first using decode-and-forward scheme at relay node and consider SPSC performance of the first user U_1 as (14).

$$\begin{aligned} G_1 = & \Pr (C_1 > 0) \\ = & \Pr \left(\min \left(SNR_R^1, SNR_{U_1} \right) > SNR_{E1} \right) \\ = & \left[\underbrace{\Pr \left(|h_{R_{n^*}}|^2 > \frac{\rho_E |h_E|^2}{\bar{\rho}_S \left(1 - \rho_E a_2 |h_E|^2 \right)}, \bar{\rho}_S < \frac{\rho_I}{|h_{SP}|^2} \right)}_{G_{1,1}} \right. \\ & \left. + \underbrace{\Pr \left(|h_{R_{n^*}}|^2 > \frac{\rho_E |h_E|^2 |h_{SP}|^2}{\rho_I \left(1 - a_2 \rho_E |h_E|^2 \right)}, \bar{\rho}_S > \frac{\rho_I}{|h_{SP}|^2} \right)}_{G_{1,2}} \right] \\ & \times \underbrace{\Pr \left(|h_{U_1}|^2 > \frac{\rho_E |h_E|^2}{\rho_R \left(1 - a_2 \rho_E |h_E|^2 \right)} \right)}_{G_{1,3}} \end{aligned} \tag{14}$$

We then compute each component $G_{1,1}, G_{1,2}, G_{1,3}$ as (15).

$$\begin{aligned}
G_{1,1} =& \Pr\left(|h_{R_{n^*}}|^2 > \frac{\rho_E |h_E|^2}{\bar{\rho}_S \left(1-\rho_E a_2 |h_E|^2\right)}, |h_E|^2 < \eta, \bar{\rho}_S < \frac{\rho_I}{|h_{SP}|^2} \right) \\
=& \int_0^{\frac{\rho_I}{\bar{\rho}_S}} f_{|h_{SP}|^2}(x) \int_0^{\eta} f_{|h_E|^2}(y) \left[1 - F_{|h_{R_{n^*}}|^2}\left(\frac{\rho_E y}{\bar{\rho}_S (1-\rho_E a_2 y)} \right) \right] dxdy \\
=& \left(1 - e^{-\frac{\rho_I}{\bar{\rho}_S \lambda_{SP}}}\right) \sum_{n=1}^{N} \left(\begin{array}{c} N \\ n \end{array} \right) \frac{(-1)^{n-1}}{\lambda_E} \int_0^{\eta} e^{-y\left(\frac{1}{\lambda_E} + \frac{n\rho_E}{\bar{\rho}_S \lambda_{SR}(1-a_2\rho_E y)}\right)} dy
\end{aligned} \tag{15}$$

where $\eta = \frac{1}{a_2 \rho_E}$.

The closed-form expression for $G_{1,1}$ is very difficult to achieve, then using the formula Gaussian-Chebyshev quadrature, $G_{1,1}$ is given as (16)

$$\begin{aligned}
G_{1,1} \approx& \left(1 - e^{-\frac{\rho_I}{\bar{\rho}_S \lambda_{SP}}}\right) \sum_{n=1}^{N} \sum_{p=1}^{P} \left(\quad \right) \frac{\eta\pi (-1)^{n-1} \sqrt{1-\varsigma_p^2}}{2P\lambda_E} \\
& \times e^{-\frac{(\varsigma_p+1)\eta}{2\lambda_E} - \frac{(\eta\varsigma_p+\eta)n\rho_E}{\bar{\rho}_S \lambda_{SR}[2-a_2\rho_E(\eta\varsigma_p+\eta)]}}
\end{aligned} \tag{16}$$

where $\varsigma_p = \cos\left(\frac{2p-1}{2P}\pi\right)$.

Next, $G_{1,2}$ is calculated as (17).

$$\begin{aligned}
G_{1,2} =& \Pr\left(|h_{R_{n^*}}|^2 > \frac{\rho_E |h_E|^2 |h_{SP}|^2}{\rho_I \left(1 - a_2\rho_E |h_E|^2\right)}, |h_E|^2 < \eta, \bar{\rho}_S > \frac{\rho_I}{|h_{SP}|^2} \right) \\
=& \int_0^{\eta} f_{|h_E|^2}(x) \int_{\frac{\rho_I}{\bar{\rho}_S}}^{\infty} f_{|h_{SP}|^2}(y) \left[1 - F_{|h_{R_{n^*}}|^2}\left(\frac{\rho_E xy}{\rho_I (1-a_2\rho_E x)} \right) \right] dxdy \\
=& \sum_{n=1}^{N} \left(\begin{array}{c} N \\ n \end{array} \right) \frac{(-1)^{n-1}}{\lambda_{SP}\lambda_E} \int_0^{\eta} e^{-\frac{x}{\lambda_E}} \int_{\frac{\rho_I}{\bar{\rho}_S}}^{\infty} e^{-y\left(\frac{1}{\lambda_{SP}} + \frac{n\rho_E x}{\rho_I (1-a_2\rho_E x)\lambda_{SR}}\right)} dxdy \\
=& \sum_{n=1}^{N} \left(\begin{array}{c} N \\ n \end{array} \right) \frac{(-1)^{n-1}}{\lambda_{SP}\lambda_E} \int_0^{\eta} e^{-\frac{x}{\lambda_E} - \frac{\rho_I}{\bar{\rho}_S}\left(\frac{1}{\lambda_{SP}} + \frac{n\rho_E x}{\rho_I(1-a_2\rho_E x)\lambda_{SR}}\right)} \\
& \times \left(\frac{1}{\lambda_{SP}} + \frac{n\rho_E x}{\rho_I (1-a_2\rho_E x)\lambda_{SR}} \right)^{-1} dx
\end{aligned} \tag{17}$$

Keep using the formula Gaussian-Chebyshev quadrature, $G_{1,2}$ is given by (18)

$$G_{1,2} \approx \sum_{n=1}^{N} \sum_{v=1}^{V} \left(\quad \right) \frac{\eta\pi(-1)^{n-1}\sqrt{1-\upsilon_v^2}}{2V\lambda_{SP}\lambda_E \Phi(w)} e^{-\frac{(\upsilon_v+1)\eta}{2\lambda_E} - \frac{\rho_I \Phi(\upsilon_v)}{\bar{\rho}_S}} \tag{18}$$

where $\upsilon_v = \cos\left(\frac{2v-1}{2V}\pi\right)$ and $\Phi(w) = \left(\frac{1}{\lambda_{SP}} + \frac{n\rho_E(\eta w+\eta)}{[2-a_2\rho_E(\eta w+\eta)]\rho_I\lambda_{SR}} \right)$.

Next, $G_{1,3}$ is calculated as (19)

$$\begin{aligned} G_{1,3} =& \Pr\left(|h_{U_1}|^2 > \frac{\rho_E |h_E|^2}{\rho_R \left(1 - a_2 \rho_E |h_E|^2\right)}, |h_E|^2 < \eta \right) \\ =& \int_0^{\eta} f_{|h_E|^2}(x) \left[1 - F_{|h_{U_1}|^2}\left(\frac{\rho_E x}{\rho_R (1 - a_2 \rho_E x)}\right)\right] dx \\ =& \frac{1}{\lambda_E} \int_0^{\eta} e^{-x\left(\frac{1}{\lambda_E} + \frac{\rho_E}{\lambda_{U_1} \rho_R (1 - a_2 \rho_E x)}\right)} dx \end{aligned} \tag{19}$$

Keep using the formula Gaussian-Chebyshev quadrature, $G_{1,3}$ is given by (20)

$$G_{1,3} \approx \frac{\pi\eta}{2\lambda_E Q} \sum_{q=1}^{Q} \sqrt{1 - \varsigma_q^2} e^{-\frac{(\varsigma_q+1)\eta}{2\lambda_E} - \frac{(\varsigma_q+1)\rho_E \eta}{\lambda_{U_1} \rho_R [2 - (\varsigma_q+1) a_2 \rho_E \eta]}} \tag{20}$$

where $\varsigma_q = \cos\left(\frac{2q-1}{2Q}\pi\right)$.

Substituting (20), (18) and (16) into (14), G_1 is given by (21)

$$\begin{aligned} G_1 =& \Bigg[\left(1 - e^{-\frac{\rho_I}{\bar{\rho}_S \lambda_{SP}}}\right) \sum_{n=1}^{N} \sum_{p=1}^{P} \binom{N}{n} \frac{\eta\pi(-1)^{n-1}\sqrt{1 - \varsigma_p^2}}{2P\lambda_E} \\ &\times e^{-\frac{(\varsigma_p+1)\eta}{2\lambda_E} - \frac{(\eta\varsigma_p+\eta) n \rho_E}{\bar{\rho}_S \lambda_{SR}[2 - a_2 \rho_E (\eta\varsigma_p+\eta)]}} \\ &+ \sum_{n=1}^{N} \sum_{v=1}^{V} \binom{N}{n} \frac{\eta\pi(-1)^{n-1}\sqrt{1 - \upsilon_v^2}}{2V\lambda_{SP}\lambda_E \Phi(w)} e^{-\frac{(\upsilon_v+1)\eta}{2\lambda_E} - \frac{\rho_I \Phi(\upsilon_v)}{\bar{\rho}_S}} \Bigg] \\ &\times \frac{\pi\eta}{2\lambda_E Q} \sum_{q=1}^{Q} \sqrt{1 - \varsigma_q^2} e^{-\frac{(\varsigma_q+1)\eta}{2\lambda_E} - \frac{(\varsigma_q+1)\rho_E \eta}{\lambda_{U_1} \rho_R [2 - (\varsigma_q+1) a_2 \rho_E \eta]}} \end{aligned} \tag{21}$$

3.2. SPSC computation at U_2

In similar way, SPSC of user U_2 is expressed by (22)

$$\begin{aligned} G_2 =& \Pr(C_2 > 0) \\ =& \Pr\left(\min\left(SNR_R^2, SNR_{U_2,x_2}\right) > SNR_{E2}\right) \\ =& \Bigg[\underbrace{\Pr\left(|h_{R_{n^*}}|^2 > \bar{a} a_2 \rho_E |h_E|^2, |h_{SP}|^2 < \frac{\rho_I}{\bar{\rho}_S} \right)}_{G_{2,1}} \\ &+ \underbrace{\Pr\left(|h_{R_{n^*}}|^2 > \tilde{a} a_2 \rho_E |h_E|^2 |h_{SP}|^2, |h_{SP}|^2 > \frac{\rho_I}{\bar{\rho}_S} \right)}_{G_{2,2}} \Bigg] \\ &\times \underbrace{\Pr\left(|h_{U_2}|^2 > \frac{\rho_E |h_E|^2}{\rho_R} \right)}_{G_{2,3}} \end{aligned} \tag{22}$$

where $\bar{a} = \frac{1}{a_2 \bar{\rho}_S}$ and $\tilde{a} = \frac{1}{a_2 \rho_I}$. These terms $G_{2,1}, G_{2,2}, G_{2,3}$ are respectively formulated by (23) and (24)

$$\begin{aligned}
G_{2,1} =& \Pr\left(|h_{R_{n^*}}|^2 > \bar{a}a_2\rho_E|h_E|^2, |h_{SP}|^2 < \frac{\rho_I}{\bar{\rho}_S}\right)\\
=& \int_0^{\frac{\rho_I}{\bar{\rho}_S}} f_{|h_{SP}|^2}(x) \int_0^{\infty} f_{|h_E|^2}(y) \left[1 - F_{|h_{R_{n^*}}|^2}(\bar{a}a_2\rho_E y)\right] dxdy\\
=& \left(1 - e^{-\frac{\rho_I}{\bar{\rho}_S\lambda_{SP}}}\right) \sum_{n=1}^{N} \left(\begin{array}{c} N \\ n \end{array}\right) \frac{(-1)^{n-1}}{\lambda_E} \int_0^{\infty} e^{-y\left(\frac{1}{\lambda_E} + \frac{n\bar{a}a_2\rho_E}{\lambda_{SR}}\right)} dy\\
=& \left(1 - e^{-\frac{\rho_I}{\bar{\rho}_S\lambda_{SP}}}\right) \sum_{n=1}^{N} \left(\begin{array}{c} N \\ n \end{array}\right) \frac{(-1)^{n-1}\lambda_{SR}}{\lambda_{SR} + n\lambda_E\bar{a}a_2\rho_E}
\end{aligned} \tag{23}$$

$$\begin{aligned}
G_{2,2} =& \Pr\left(|h_{R_{n^*}}|^2 > \tilde{a}a_2\rho_E|h_E|^2|h_{SP}|^2, |h_{SP}|^2 > \frac{\rho_I}{\bar{\rho}_S}\right)\\
=& \int_0^{\infty} f_{|h_E|^2}(x) \int_{\frac{\rho_I}{\bar{\rho}_S}}^{\infty} f_{|h_{SP}|^2}(y) \left[1 - F_{|h_{R_{n^*}}|^2}(\tilde{a}a_2\rho_E xy)\right] dxdy\\
=& \sum_{n=1}^{N} \left(\begin{array}{c} N \\ n \end{array}\right) \frac{\lambda_{SR}(-1)^{n-1} e^{-\frac{\rho_I}{\bar{\rho}_S\lambda_{SP}}}}{na_2\tilde{a}\rho_E\lambda_E\lambda_{SP}} \int_0^{\infty} \frac{e^{-\ell_n x}}{\varpi_n + x} dx
\end{aligned} \tag{24}$$

where $\ell_n = \frac{1}{\lambda_E} + \frac{n\tilde{a}a_2\rho_E}{\lambda_{SR}}$ and $\varpi_n = \frac{\lambda_{SR}}{\lambda_{SP}n\tilde{a}a_2\rho_E}$.

We are using [[25], 8.211.1], $G_{2,2}$ is given by (25).

$$G_{2,2} = \sum_{n=1}^{N} \left(\begin{array}{c} N \\ n \end{array}\right) \frac{\lambda_{SR}(-1)^n e^{-\frac{\rho_I}{\bar{\rho}_S\lambda_{SP}} + \ell_n\varpi_n}}{na_2\tilde{a}\rho_E\lambda_E\lambda_{SP}} Ei\left(-\ell_n\varpi_n\right) \tag{25}$$

Next, we are calculated $G_{2,3}$ as (26).

$$\begin{aligned}
G_{2,3} =& \Pr\left(|h_{U_2}|^2 > \frac{\rho_E|h_E|^2}{\rho_R}\right)\\
=& \int_0^{\infty} f_{|h_E|^2}(x) \left[1 - F_{|h_{U_2}|^2}\left(\frac{\rho_E x}{\rho_R}\right)\right] dx\\
=& \frac{1}{\lambda_E} \int_0^{\infty} e^{-x\left(\frac{1}{\lambda_E} + \frac{\rho_E}{\rho_R\lambda_{U_2}}\right)} dx\\
=& \frac{\rho_R\lambda_{U_2}}{\rho_R\lambda_{U_2} + \lambda_E\rho_E}
\end{aligned} \tag{26}$$

Substituting (26), (25) and (23) into (22), G_2 is given by (27).

$$\begin{aligned}
G_2 =& \sum_{n=1}^{N} \left(\begin{array}{c} N \\ n \end{array}\right) \frac{\rho_R\lambda_{U_2}\lambda_{SR}}{\rho_R\lambda_{U_2} + \lambda_E\rho_E} \left[\left(1 - e^{-\frac{\rho_I}{\bar{\rho}_S\lambda_{SP}}}\right) \frac{(-1)^{n-1}}{\lambda_{SR} + n\lambda_E\bar{a}a_2\rho_E}\right.\\
&\left. + \frac{(-1)^n e^{-\frac{\rho_I}{\bar{\rho}_S\lambda_{SP}} + \ell_n\varpi_n}}{na_2\tilde{a}\rho_E\lambda_E\lambda_{SP}} Ei\left(-\ell_n\varpi_n\right)\right]
\end{aligned} \tag{27}$$

4. NUMERICAL RESULTS

Our simulation parameters here are $a_1 = 0.7$ and $a_2 = 0.3$. $N = 2$, $R_1 = R_2 = 1$. $\rho_I = 5\,dB.\rho_E = 15\,dB$. $\lambda_{SP} = 0.1$, $\lambda_{SR} = 1$, $\lambda_{RD1} = 0.9$, $\lambda_{RD2} = 0.6$ and $\lambda_{RE} = 0.1$. $Q = V = 1000$.

Figure 2 depicts SPSC performance versus transmit SNR. We consider many cases related to CR-NOMA for $\rho_E = 5, 10, 15(dB)$. It is very high value of SPSC when increasing ρ to 20 (dB) and greater. Signal x_2 provides better SPSC performance compared with signal x_2, and it can be explained that different power allocated to each signal. Comparing the simulation results with the analytical results, there are tight matching curves.

It can be seen how the number of the relay nodes make impacts on SPSC performance at Figure 3. Similar trend of SPSC can be reported in Figure 3, it means SPSC will be worse as increasing ρ to 30 (dB). Figure 3 depicts SPSC curves is highest at $N = 15$. When ρ is greater than 25 (dB), SPSC curves meet saturation.

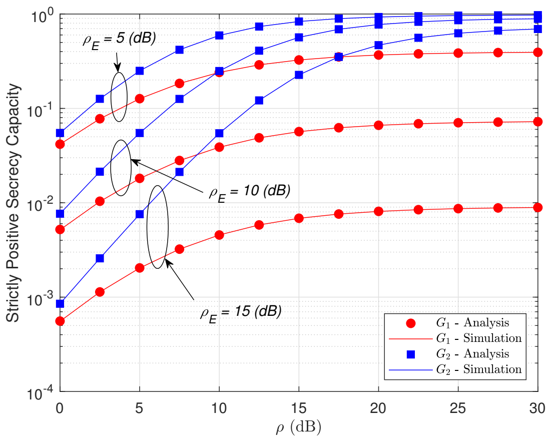

Figure 2.
SPSC versus transmit SNR at BS

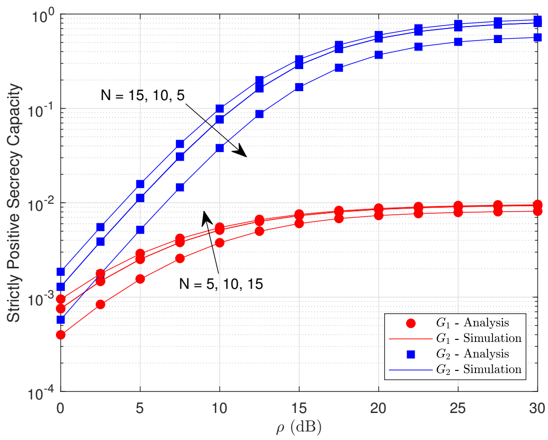

Figure 3. SPSC versus transmit SNR at BS with different number of relay nodes

5. CONCLUSION

The paper studied SPSC in cognitive radio newtwork using NOMA and relay selection. Secure performance is considered as existence of an eavesdropper and acceptable SPSC can be known. Moreover, the approximate expressions in term of SPSC are derived to exhibit performance of two destinations. The derivations and analysis results showed that the proposed relay selection in CR-NOMA can effectively enhance the secure performance.

REFERENCES

[1] Dinh-Thuan Do and M.-S. Van Nguyen, "Device-to-device transmission modes in NOMA network with and without Wireless Power Transfer," *Computer Communications*, Vol. 139, pp. 67-77, May 2019.

[2] Y. Liu, Z. Qin, M. Elkashlan, Y. Gao, and L. Hanzo, "Enhancing the Physical Layer Security of Non-Orthogonal Multiple Access in LargeScale Networks," *IEEE Trans. Wirel. Commun.*, vol. 16, no. 3, pp. 1656-1672, Mar. 2017.

[3] Y. Feng, Z. Yang, and S. Yan, "Non-orthogonal multiple access and artificial-noise aided secure transmission in FD relay networks," *in Proc. IEEE GLOBECOM Wkshps*, pp. 1-6, Dec. 2017.

[4] L. Lv, Z. Ding, Q. Ni, and J. Chen, "Secure MISO-NOMA transmission with artificial noise," *IEEE Trans. on Vehic. Tech.*, vol. 67, no. 7, pp. 6700-6705, Jul. 2018.

[5] D.-T. Do, M. Vaezi, and T.-L. Nguyen, "Wireless Powered Cooperative Relaying using NOMA with Imperfect CSI," in *Proc. of IEEE Globecom Workshops (GC Wkshps)*, Abu Dhabi, UAE, pp. 1-6, 2018.

[6] D.-T. Do and A.-T. Le, "NOMA based cognitive relaying: Transceiver hardware impairments, relay selection policies and outage performance comparison," *Computer Communications*, vol. 146, pp. 144-154, 2019.

[7] D.-T. Do, A.-T. Le, and B.-M. Lee, ”On Performance Analysis of Underlay Cognitive Radio-Aware Hybrid OMA/NOMA Networks with Imperfect CSI,” *Electronics*, vol. 8, no. 7, p. 819, 2019.

[8] D.-T. Do, A.-T. Le, C.-B. Le, and B. M. Lee ”On Exact Outage and Throughput Performance of Cognitive Radio based Non-Orthogonal Multiple Access Networks With and Without D2D Link,” *Sensors (Basel)*, vol. 19, no. 15, p. 3314, 2019.

[9] T.-L. Nguyen and Dinh-Thuan Do, ”Exploiting Impacts of Intercell Interference on SWIPT-assisted Non-orthogonal Multiple Access ,” *Wireless Communications and Mobile Computing*, vol. 2018, pp. 1-12, 2018.

[10] Dinh-Thuan Do, M.-S. Van Nguyen, T.-A. Hoang, and M. Voznak, ”NOMA-Assisted Multiple Access Scheme for IoT Deployment: Relay Selection Model and Secrecy Performance Improvement,” *Sensors*, vol. 19, no. 3, p. 736, 2019.

[11] F. Zhou, et al., ”Robust AN-Aided beamforming and power splitting design for secure MISO cognitive radio with SWIPT,” *IEEE Trans. Wireless Commun.*, vol. 16, no. 4, pp. 2450-2464, Apr. 2017.

[12] H. Wang and X. Xia, ”Enhancing wireless secrecy via cooperation: signal design and optmization,” *IEEE Commun. Magz.*, vol. 53, no. 12, pp. 47-53, 2015.

[13] E. Boshkovska, et al., ”Robust resource allocation for MIMO wireless powered communication networks based on a non-linear EH model,” *IEEE Trans. Commun.*, vol. 65, no. 5, pp. 1984-1999, May 2017.

[14] E. Boshkovska, et al., ”Secure SWIPT networks based on a non-linear energy harvesting model,” *in Proc. IEEE WCNC 2017*, San Francisco, CA, USA, 2017.

[15] X. Chen, et al., ”A survey on multiple-antenna techniques for physical layer security,” *IEEE Commun. Surveys Tuts.*, vol. 19, no. 2, pp. 1027-1053, 2017.

[16] Y. Liu, et al., ”Phsical layer security for next generation wireless networks: Theories, tehcniques, and challenges,” *IEEE Commun. Surveys Tuts.*, vol. 19, no. 1, pp. 347-376, 2017

[17] Y. Sun, D. W. K. Ng, Z. Ding, and R. Schober, ”Optimal joint power and subcarrier allocation for full-duplex multicarrier non-orthogonal multiple access systems,” *IEEE Trans. Commun.*, vol. 65, no. 3, pp. 1077-1091, 2017.

[18] H. Zhang, H. Xing, J. Cheng, A. Nallanathan, and V. C. M. Leung, ”Secure resource allocation for OFDMA two-way relay wireless sensor networks without and with cooperative jamming,” *IEEE Trans. Ind. Informat.*, vol. 12, no. 5, pp. 1714-1725, Oct. 2016.

[19] Y. Wu, A. Khisti, C. Xiao, G. Caire, K.-K. Wong, and X. Gao, ”A survey of physical layer security techniques for 5g wireless networks and challenges ahead,” *IEEE J. Sel. Areas Commun.*, vol. 36, no. 4, pp. 679-695, Apr. 2018.

[20] Y. Deng, L. Wang, M. Elkashlan, A. Nallanathan, and R. K. Mallik, ”Physical layer security in three-tier wireless sensor networks: A stochastic geometry approach,” *IEEE Trans. Inf. Forensics Security*, vol. 11, no. 6, pp. 1128-1138, Jun. 2016.

[21] F. Zhu and M. Yao, ”Improving physical-layer security for CRNs using SINR-based cooperative beamforming,” *IEEE Trans. Veh. Technol.*, vol. 65, no. 3, pp. 1835-1841, Mar. 2016.

[22] A. Al-Nahari, G. Geraci, M. Al-Jamali, M. H. Ahmed, and N. Yang, ”Beamforming with artificial noise for secure MISOME cognitive radio transmissions,” *IEEE Trans. Inf. Forensics Security*, vol. 13, no. 8, pp. 1875-1889, Aug. 2018.

[23] P. Yan, Y. Zou, and J. Zhu, ”Energy-aware multiuser scheduling for physical-layer security in energy-harvesting underlay cognitive radio systems,” *IEEE Trans. Veh. Technol.*, vol. 67, no. 3, pp. 2084-2096, Mar. 2018.

[24] H. Lei, M. Xu, I. S. Ansari, G. Pan, K. A. Qaraqe, and M.-S. Alouini, ”On secure underlay MIMO cognitive radio networks with energy harvesting and transmit antenna selection,” *IEEE Trans. Green Commun. Netw.*, vol. 1, no. 2, pp. 192-203, Jun. 2017.

[25] I. S. Gradshteyn and I. M. Ryzhik, ”Table of Integrals, Series and Products,” 6th ed. New York, NY, USA: Academic Press, 2000.